

Wladek Walukiewicz

*Lawrence Berkeley National Laboratory, Berkeley CA
In collaboration with EMAT-Solar group
<http://emat-solar.lbl.gov/>*

Valence Band Anticrossing in III-Bi-V Alloys



J. Ager, **K. M. Yu**, Liliental-Weber, J. Denlinger, O. Dubon,
E. E. Haller, J. Wu
LBNL and UC Berkeley

K. Alberi, X. Li, D. Speaks, M. Mayer, R. Broesler, A.
Levander
Students, UC Berkeley

Berkeley
University of California

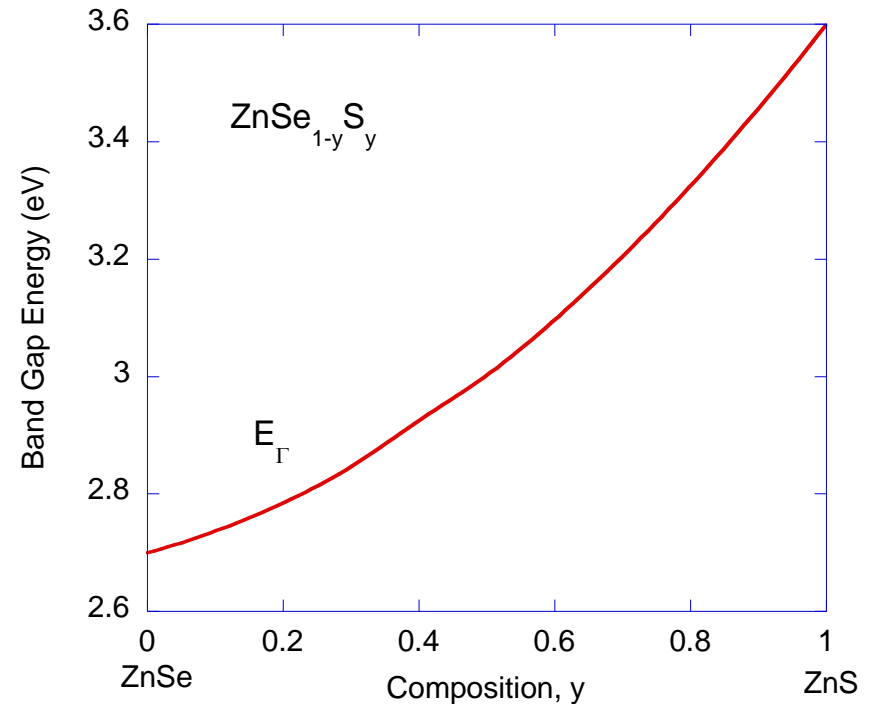
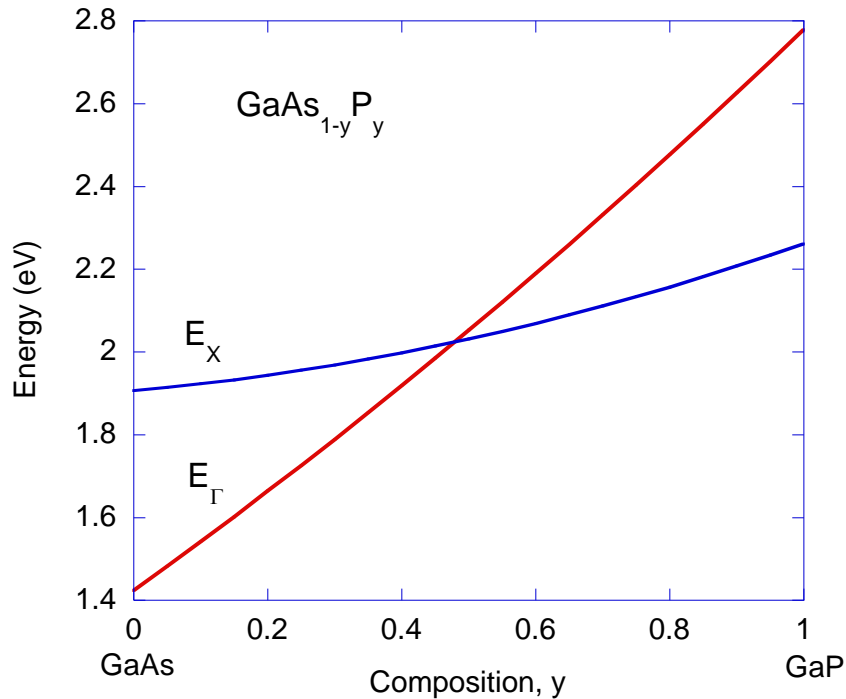
Collaborations

- **J. Geisz**, NREL (InGaAs(N))
- **C. Tu**, UCSD (GaP(N), InP(N))
- **C. Skierbiszewski**, Unipres (InGaAs(N))
- **A. Ramdas**, Purdue University (ZnTe(Se), ZnTe(S)..)
- **I. K. Sou**, UST, Hong Kong (ZnSe(Te), ZnS(Te))
- **I. Suemune**, (Hokkaido University) (InGaAs(N))
- **T. Kuech**, University of Wisconsin (GaN(As))
- **Y. Nabetani**, University of Yamanashi (ZnSe(O), ZnTe(O))
- **J. A Gupta**, NRC, Canada (GaAs(Sb))
- **S. Watkins**, Simon Frasier (GaAs(Sb))
- **A. Krotkus**, SRI, Vilnius (GaAs(Bi))
- **J. Blacksberg**, JPL (Ge(Sn))
- **T. Foxon, S. Novikov**, University of Nottingham (GaN(As))
- **J. Furdyna**, University of Notre Dame (GaAs(Mn))

Outline

- Highly Mismatched Semiconductor Alloys
- Conduction and Valence Band Anticrossing
- Key examples of highly mismatched alloys (HMAs)
 - $\text{GaN}_x\text{As}_{1-x}$
 - $\text{ZnO}_x\text{Se}_{1-x}$
- Group III-Bi-V highly mismatched alloys
- Electronic Band Structure Engineering of HMAs
- Potential applications of HMAs (including bismides)
- Conclusions and outlook

Normal alloying: well matched alloys



Relatively easy to grow in the whole composition range

Small deviations from linear interpolation between end point compounds

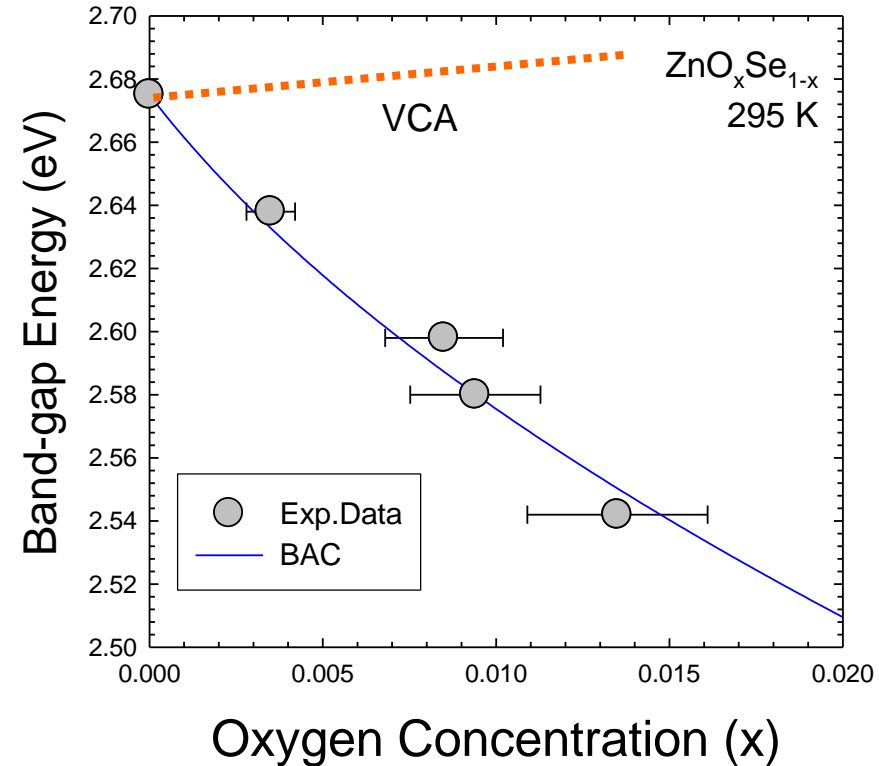
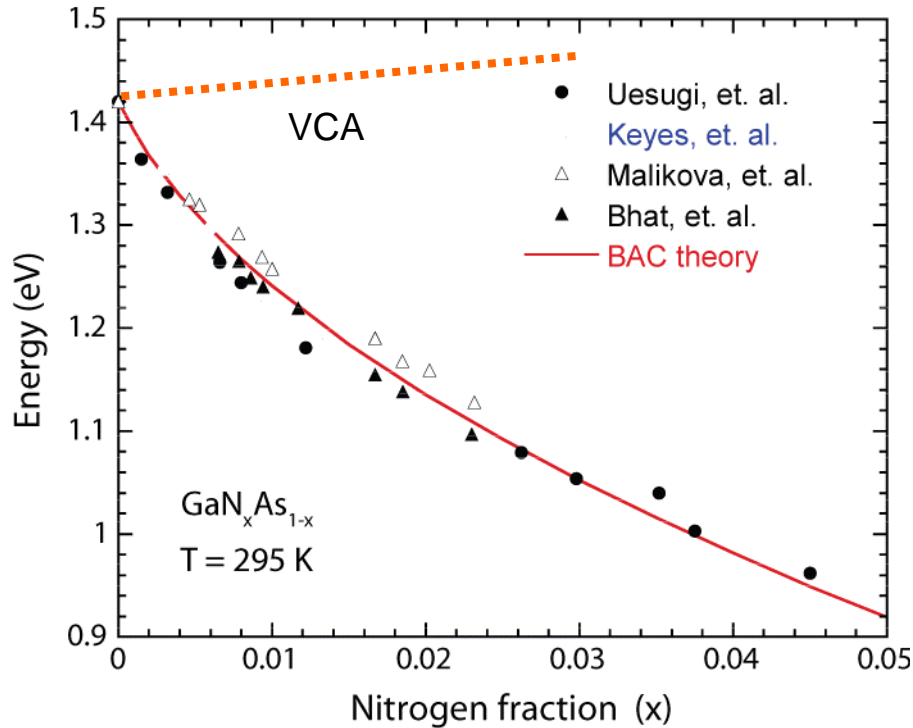
Anion Site Alloys

Electronegativities, X and atomic radii, R

IV	V	VI
C 2.6	N X=3.0 R=0.075 nm	O X=3.4 R=0.073 nm
Si 1.9	P X=2.2 R=0.12 nm	S X=2.6 R=0.11 nm
Ge 1.9	As X=2.2 R=0.13 nm	Se X=2.6 R=0.12 nm
Sn 2.0	Sb 2.1 R=0.14 nm	Te 2.1 R=0.14 nm

- A large variety of potential alloys.
- Well matched alloys: replacing atoms with similar properties
- What happens when As is replaced with very much different N or Se with O?

III-Vs and II-VIs HMAs



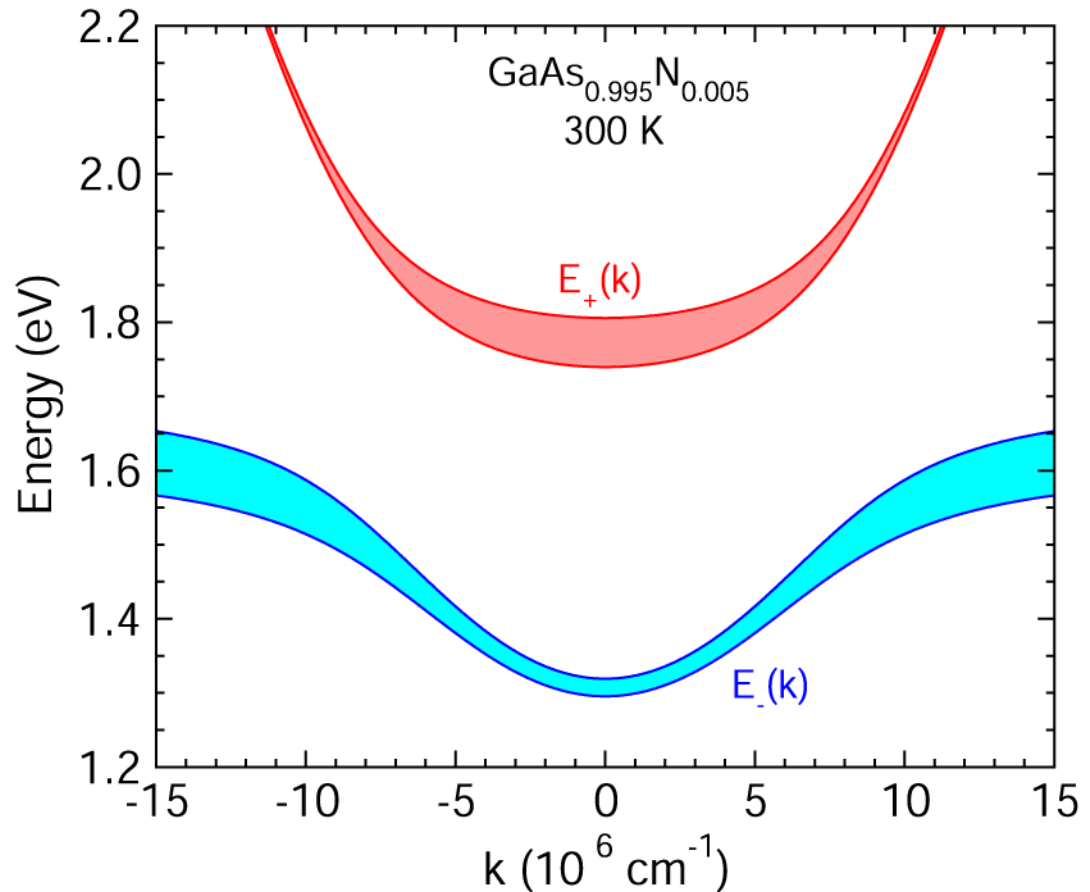
Drastic deviation from linear interpolation between end point compounds

W. Shan, et. al., J. Phys.: Condens Matter, **16** S3355 (2004)

W. Shan, et. al., Appl. Phys. Lett., **83**, 299 (2003)

Band Anticrossing in HMA: Dilute nitride alloys: $\text{GaAs}_{1-x}\text{N}_x$

- Interaction of localized N levels with extended states of the conduction band.
- Homogenous broadening within coherent potential approximation



$$E_{\pm}(k) = \frac{1}{2} \left\{ \left[E^C(k) + E^L \right] \pm \sqrt{\left[E^C(k) - E^L \right]^2 + 4C_{NM}^2 \cdot x} \right\}$$

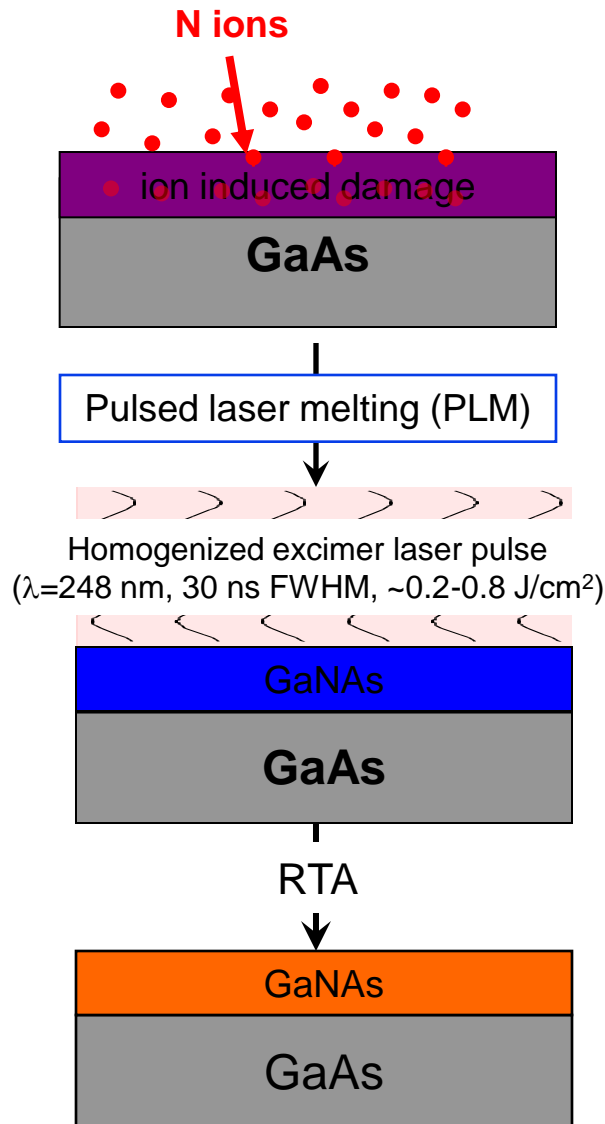
Highly mismatched Alloys

Electronegativities, X and atomic radii, R

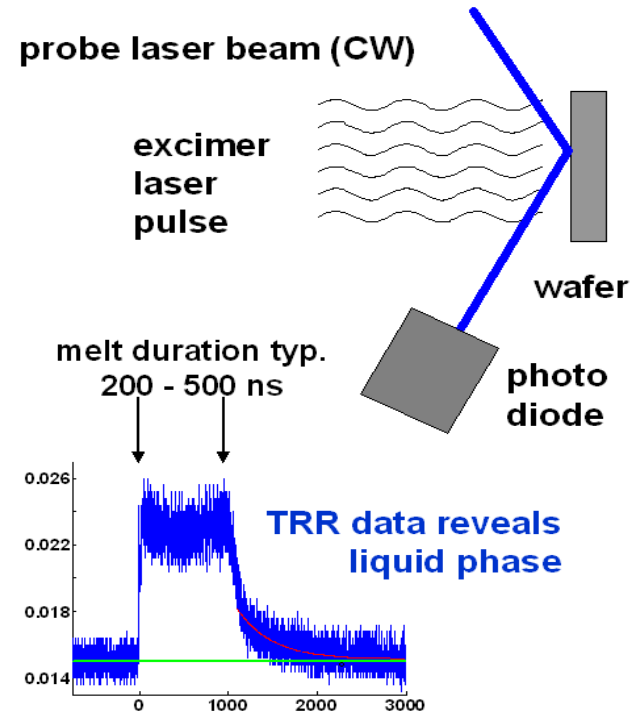
IV	V	VI
C 2.6	N X=3.0 R=0.075 nm	O X=3.4 R=0.073 nm
Si 1.9	P X=2.2 R=0.12 nm	S X=2.6 R=0.11 nm
Ge 1.9	As X=2.2 R=0.13 nm	Se X=2.6 R=0.12 nm
Sn 2.0	Sb 2.1 R=0.14 nm	Te 2.1 R=0.14 nm

- A large variety of potential highly mismatched alloys.
 $\text{III-N}_x\text{-V}_{1-x}$
 $\text{II-O}_x\text{-VI}_{1-x}$
- *Compared to normal alloys, they are difficult to synthesize*
- *Require non-equilibrium synthesis*

Synthesis of HMAs by ion implantation and pulsed laser melting (II-PLM)

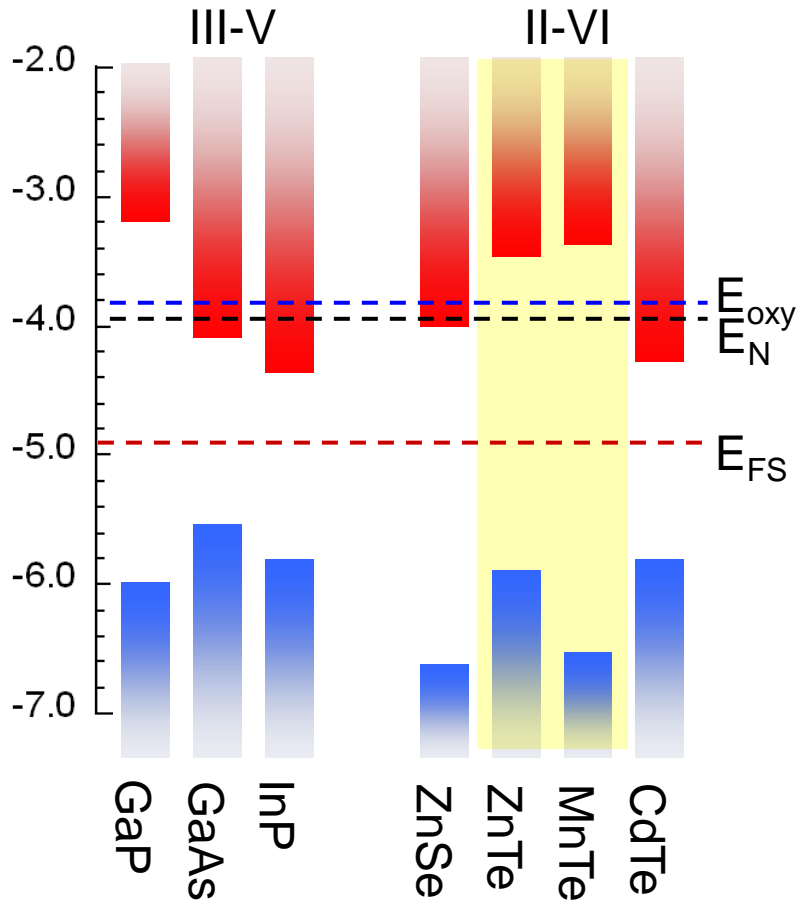


Time Resolved Reflectivity



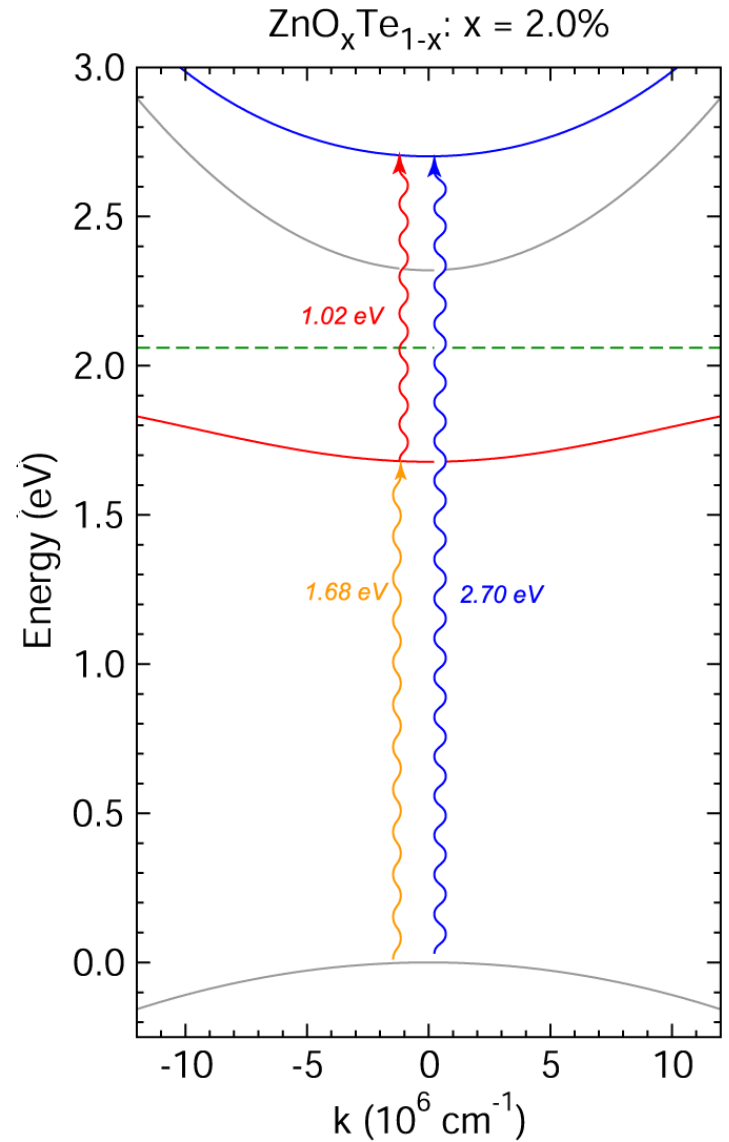
- Liquid phase epitaxy at submicrosecond time scales
- Supersaturation of implanted species
- Suppression of secondary phases

Alloys with local level below the direct CBE

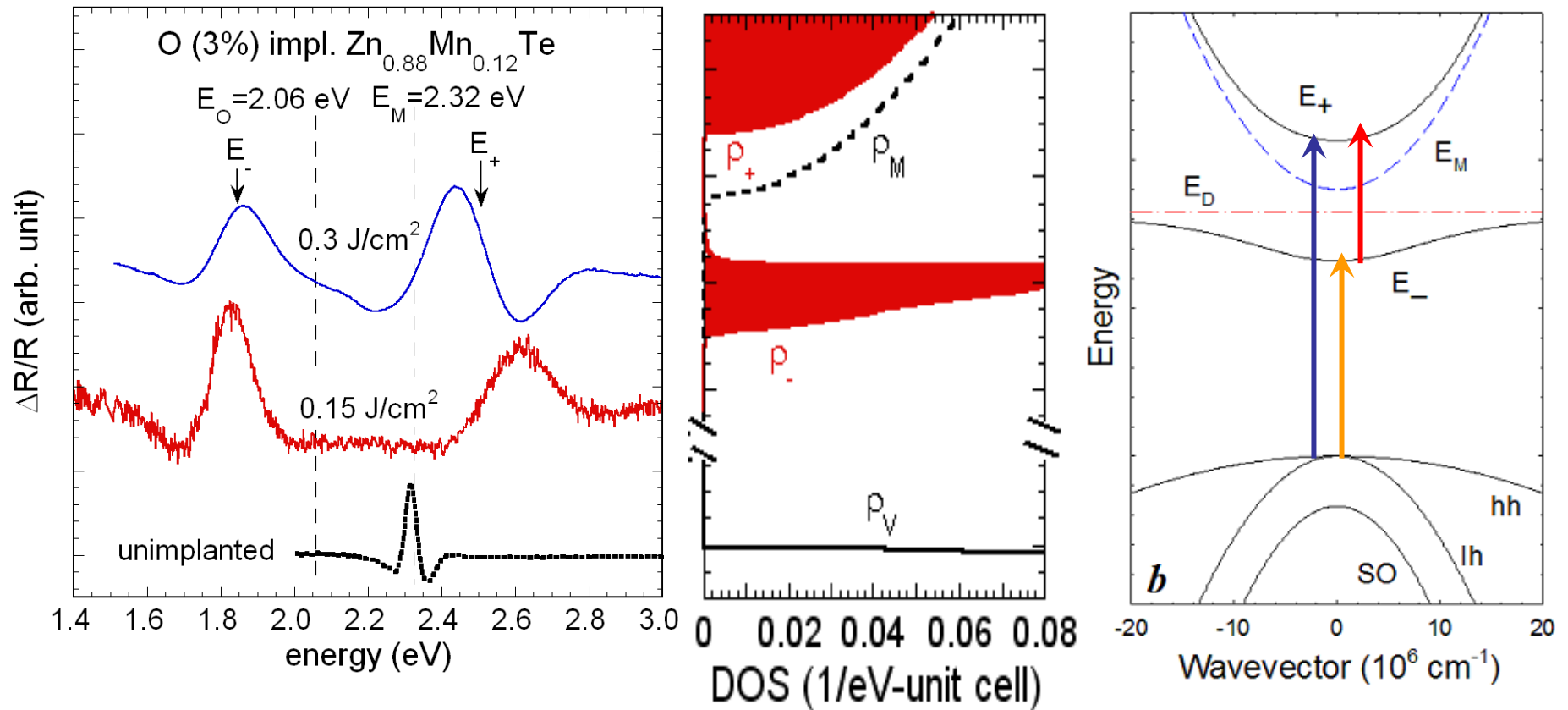


Oxygen level in ZnTe and MnTe is ~ 0.2 eV below the conduction band (CB) edge

Can it be used to form a sparate band?



Intermediate Band $\text{Zn}_{1-y}\text{Mn}_y\text{O}_x\text{Te}_{1-x}$ by PLM



- An isolated intermediate band is formed in $\text{ZnMnTe}_{1-x}\text{O}_x$

Highly Mismatched Alloy

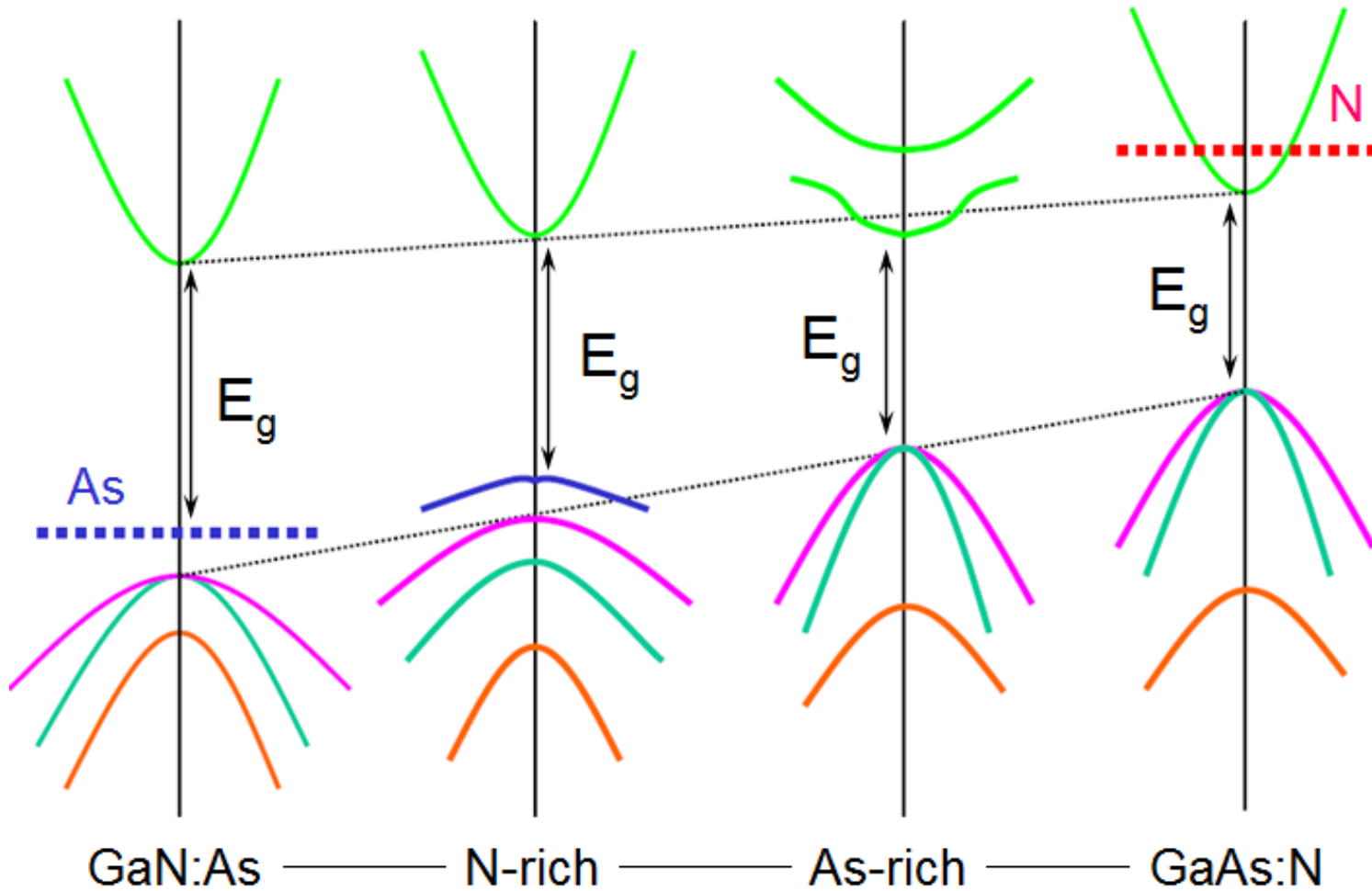
Valence Band Anticrossing (VBAC)

Electronegativities, X and atomic radii, R

IV	V	VI
C 2.6	N X=3.0 R=0.075 nm	O X=3.4 R=0.073 nm
Si 1.9	P X=2.2 R=0.12 nm	S X=2.6 R=0.11 nm
Ge 1.9	As X=2.2 R=0.13 nm	Se X=2.6 R=0.12 nm
Sn 2.0	Sb 2.1 R=0.14 nm	Te 2.1 R=0.14 nm

- Highly electronegative anions are partially replaced with more metallic isovalent atoms e. g. N-rich GaN_{1-x}As_x
- *The metallic atoms form localized states close to the valence band that interact with the valence band*

Band anticrossing in the whole composition range: GaNAs

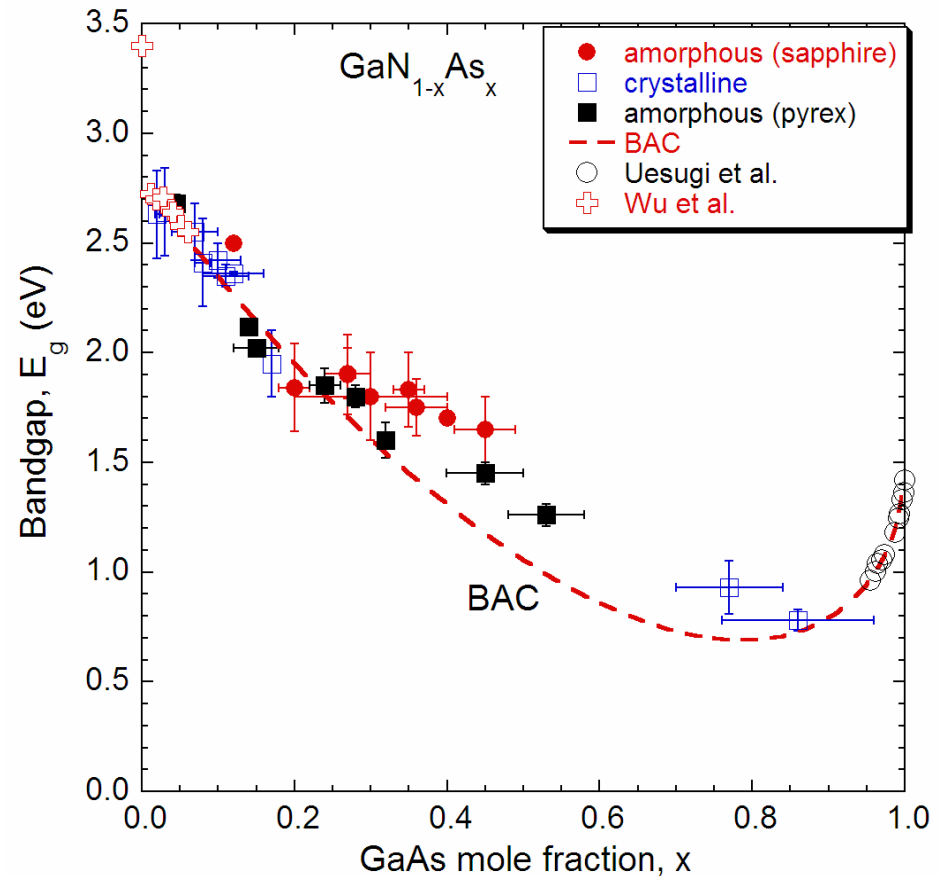


HMAs over a wide composition range

GaN_{1-x}As_x alloys over the **entire composition range** were grown by a highly non-equilibrium synthesis method: low temperatures plasma-assisted MBE

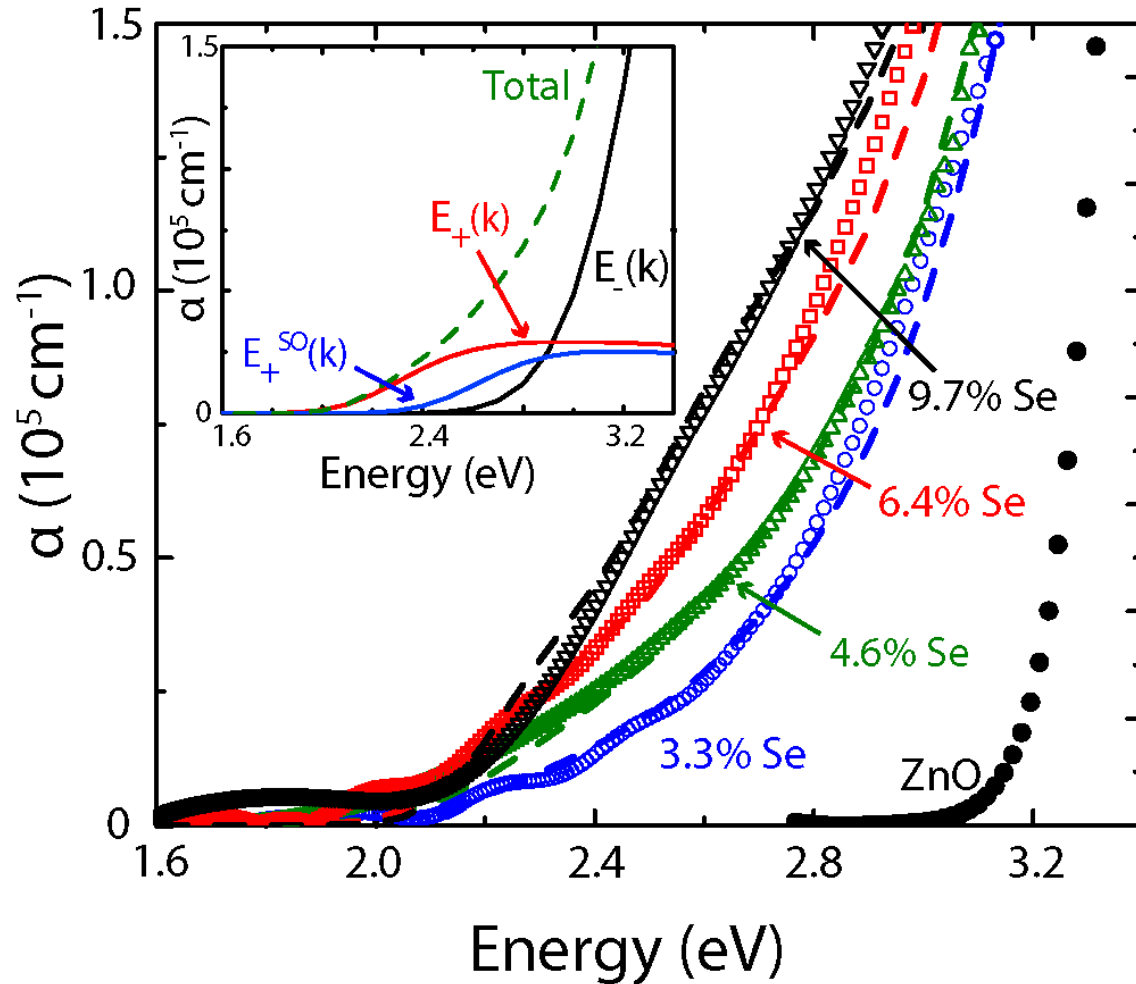
- Alloys are **amorphous** for $0.15 < x < 0.8$
- Sharp optical absorption gives well-defined bandgaps
- Bandgap and band edge **tunable** in a broad range

Red curve: BAC prediction
J. Wu, et. al.,
Phys. Rev. B **70**, 115214 (2004).



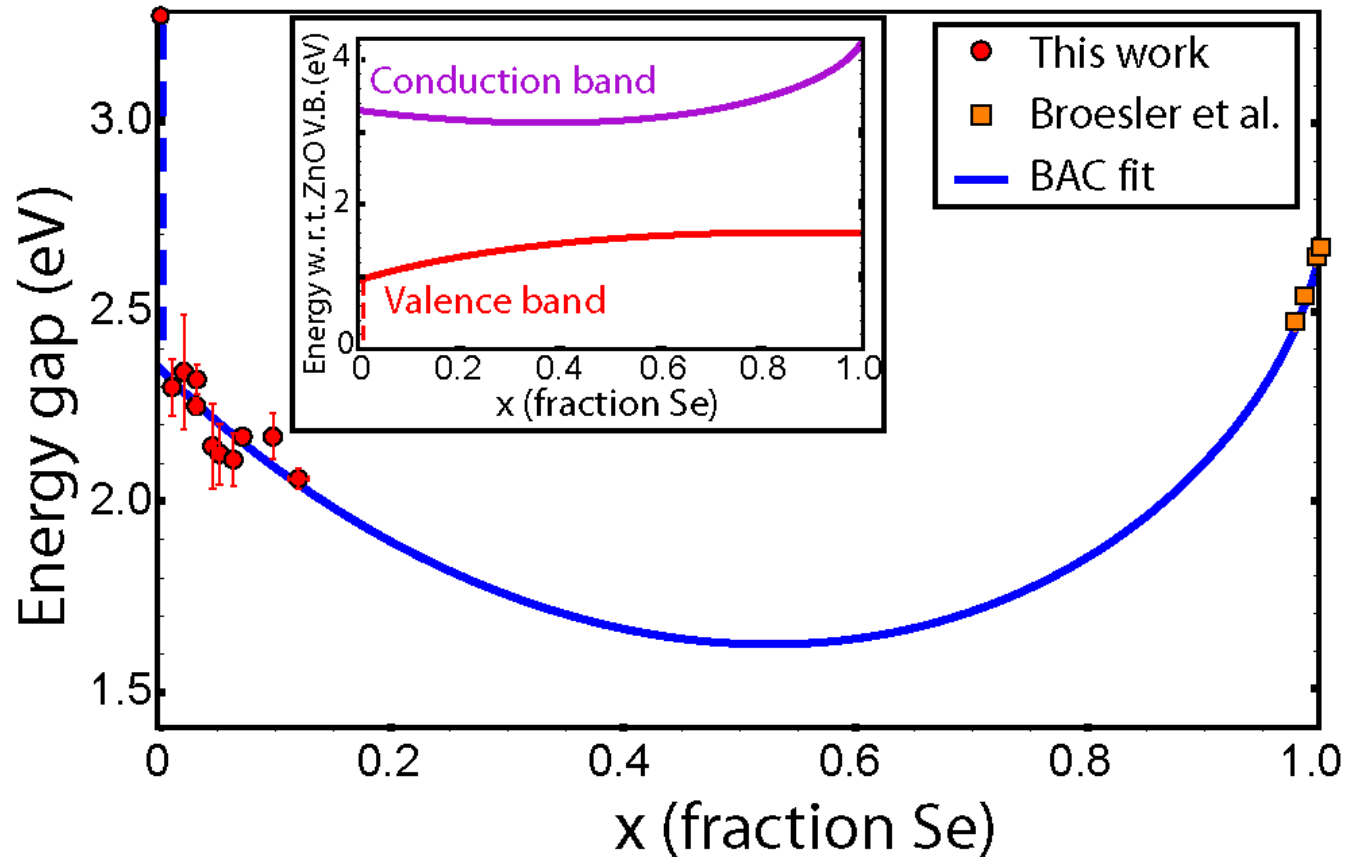


Group II-VI compound analog of $\text{GaN}_y\text{As}_{1-y}$



$$E_{\text{Se}} = E_{\text{VBM}} + 0.9 \text{ eV}, \quad C = 1.2 \text{ eV}$$

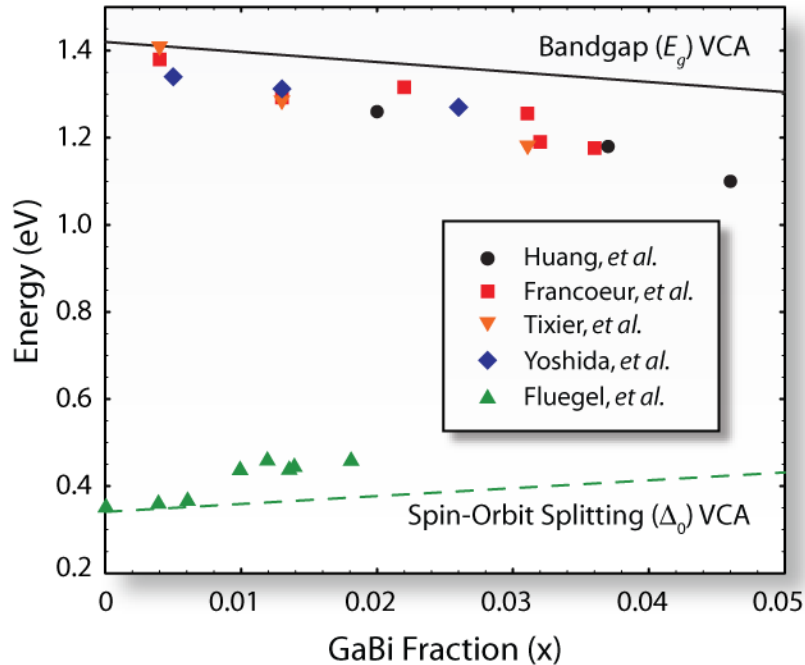
ZnO_xSe_{1-x}: Electronic Structure



Blue curve: weighted interpolation of CBAC (Se-rich) and VBAC O-rich

Optical Properties of $\text{GaBi}_x\text{As}_{1-x}$

Band gap and spin orbit splitting energies



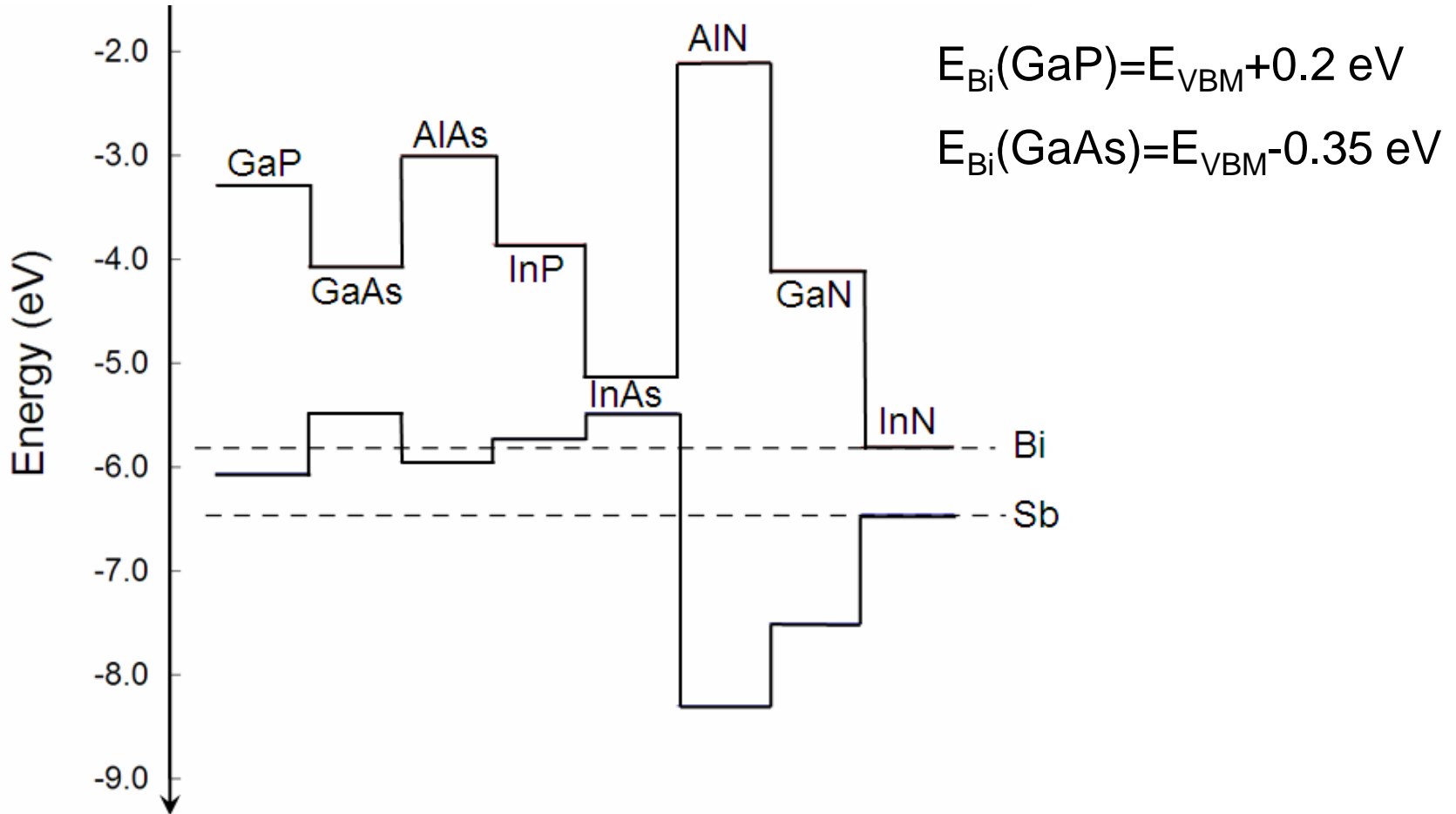
Large bandgap reduction with increase in impurity concentration

Giant spin orbit bowing*

Not readily explained by the virtual crystal approximation (VCA)

Apply a valence band anticrossing (VBAC) model to understand the origin of the bowing in bandgap and spin orbit splitting energies in $\text{GaBi}_x\text{As}_{1-x}$

Bismuth Level in III-V Compounds



Valence Band Anticrossing in $\text{GaBi}_x\text{As}_{1-x}$

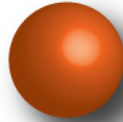
N



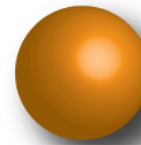
P



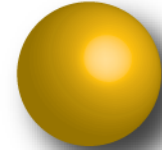
As



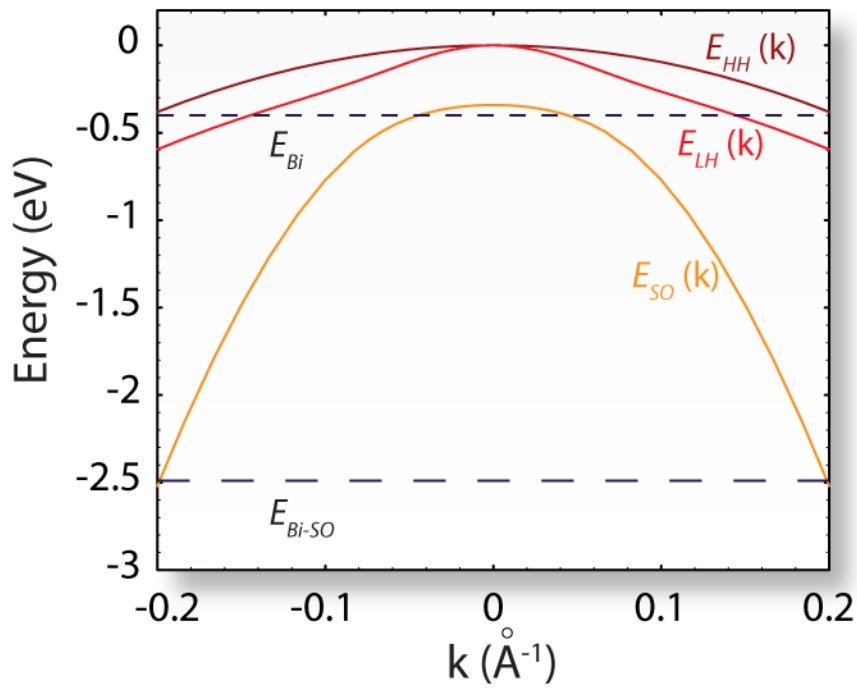
Sb



Bi



Bi Defect Levels in GaAs



Impurities of low ionization energy

Defect states located near the valence band

Anticrossing interaction between host and impurity p -like states

Bi introduces 6 p -like localized states

Valence Band Anticrossing Hamiltonian

12x12 matrix, Six valence bands and six p-symmetry impurity states

$$H_V = \begin{pmatrix} H & \alpha & \beta & 0 & \frac{i\alpha}{\sqrt{2}} & -i\sqrt{2}\beta & V(x) & 0 & 0 & 0 & 0 & 0 \\ \alpha^* & L & 0 & \beta & \frac{iD}{\sqrt{2}} & i\sqrt{\frac{3}{2}}\alpha & 0 & V(x) & 0 & 0 & 0 & 0 \\ \beta^* & 0 & L & -\alpha & -i\sqrt{\frac{3}{2}}\alpha^* & \frac{iD}{\sqrt{2}} & 0 & 0 & V(x) & 0 & 0 & 0 \\ 0 & \beta^* & -\alpha^* & H & -i\sqrt{2}\beta^* & \frac{-i\alpha^*}{\sqrt{2}} & 0 & 0 & 0 & V(x) & 0 & 0 \\ \frac{-i\alpha^*}{\sqrt{2}} & \frac{-iD}{\sqrt{2}} & i\sqrt{\frac{3}{2}}\alpha & i\sqrt{2}\beta & S & 0 & 0 & 0 & 0 & 0 & V(x) & 0 \\ i\sqrt{2}\beta^* & -i\sqrt{\frac{3}{2}}\alpha^* & \frac{-iD}{\sqrt{2}} & \frac{i\alpha}{\sqrt{2}} & 0 & S & 0 & 0 & 0 & 0 & 0 & V(x) \\ V(x) & 0 & 0 & 0 & 0 & 0 & E_{imp} & 0 & 0 & 0 & 0 & 0 \\ 0 & V(x) & 0 & 0 & 0 & 0 & 0 & E_{imp} & 0 & 0 & 0 & 0 \\ 0 & 0 & V(x) & 0 & 0 & 0 & 0 & 0 & E_{imp} & 0 & 0 & 0 \\ 0 & 0 & 0 & V(x) & 0 & 0 & 0 & 0 & 0 & E_{imp} & 0 & 0 \\ 0 & 0 & 0 & 0 & V(x) & 0 & 0 & 0 & 0 & 0 & E_{imp-so} & 0 \\ 0 & 0 & 0 & 0 & 0 & V(x) & 0 & 0 & 0 & 0 & 0 & E_{imp-so} \end{pmatrix}.$$

$$\alpha = \sqrt{3} \frac{\hbar^2}{m_0} [k_z(k_x - ik_y)\gamma_3],$$

$$\beta = \frac{\sqrt{3}}{2} \frac{\hbar^2}{m_0} [(k_x^2 - k_y^2)\gamma_2 - 2ik_x k_y \gamma_3],$$

$$V = C_A \sqrt{x}.$$

Valence Band Anticrossing Model

Interaction described by a 12 x 12 Hamiltonian

Includes

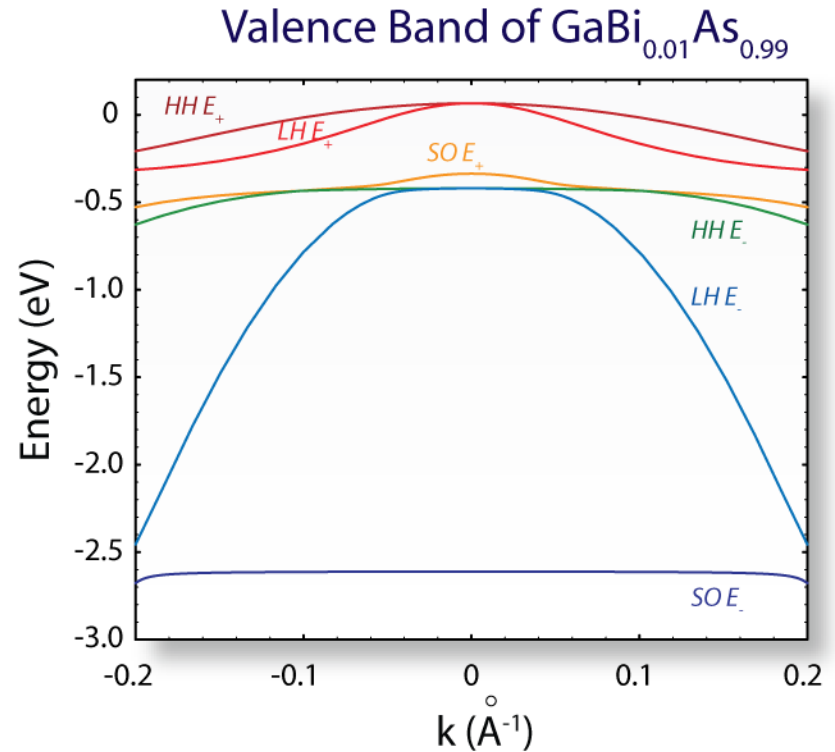
- 6 p -like states of host
- 6 p -like states of the impurity

Parameters

- Location of defect states E_{Bi} and E_{Bi-SO}
- Coupling parameter C_p (adjustable)

Restructured valence band

- HH-like (E_+ and E_-)
- LH-like (E_+ and E_-)
- SO-like (E_+ and E_-)



Photomodulated Reflectance of $\text{GaBi}_x\text{As}_{1-x}$

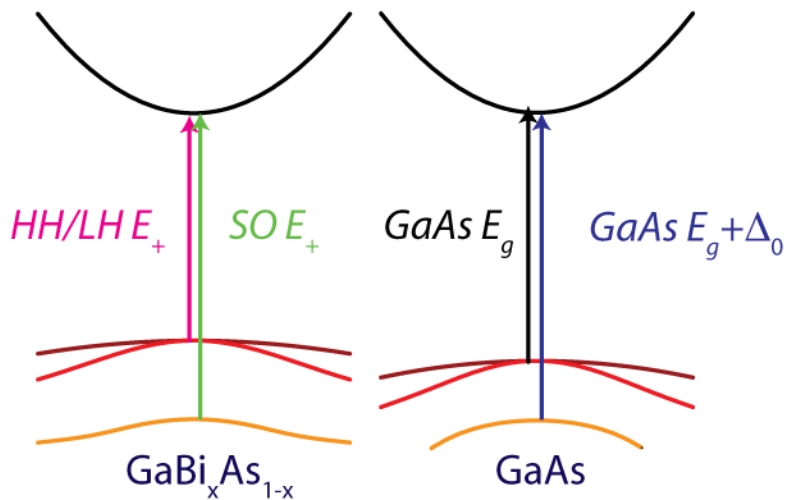
$$E_{CB} - HH/LH E_+$$

Moves downward quickly with x

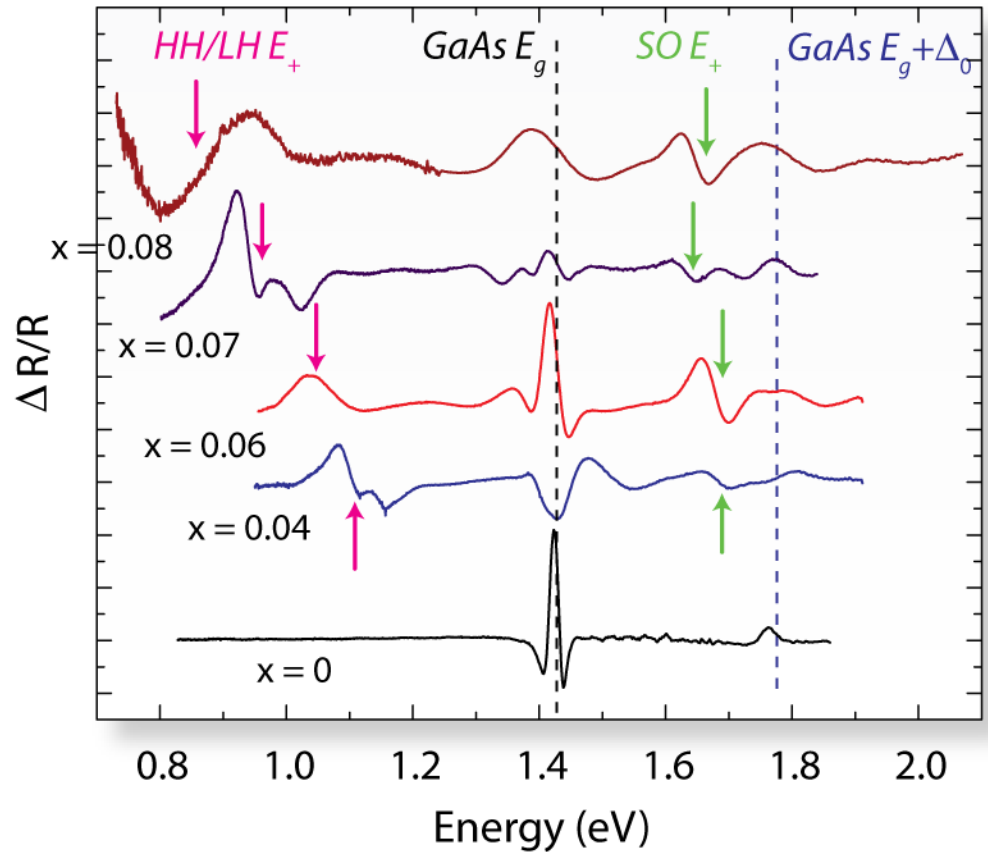
$$E_{CB} - SO E_+$$

Moves downward slowing with x

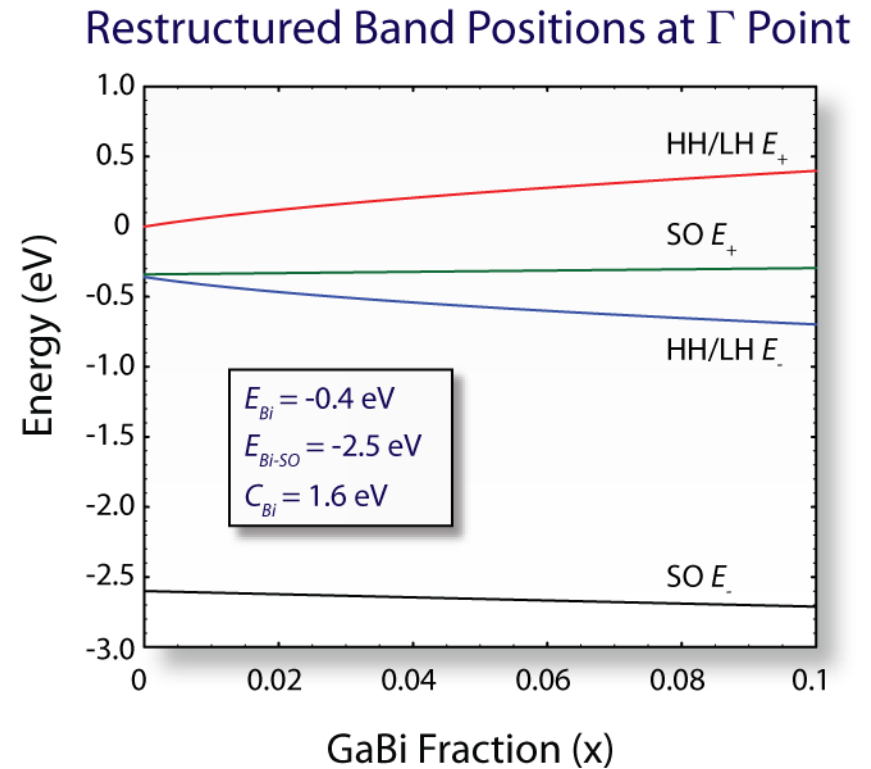
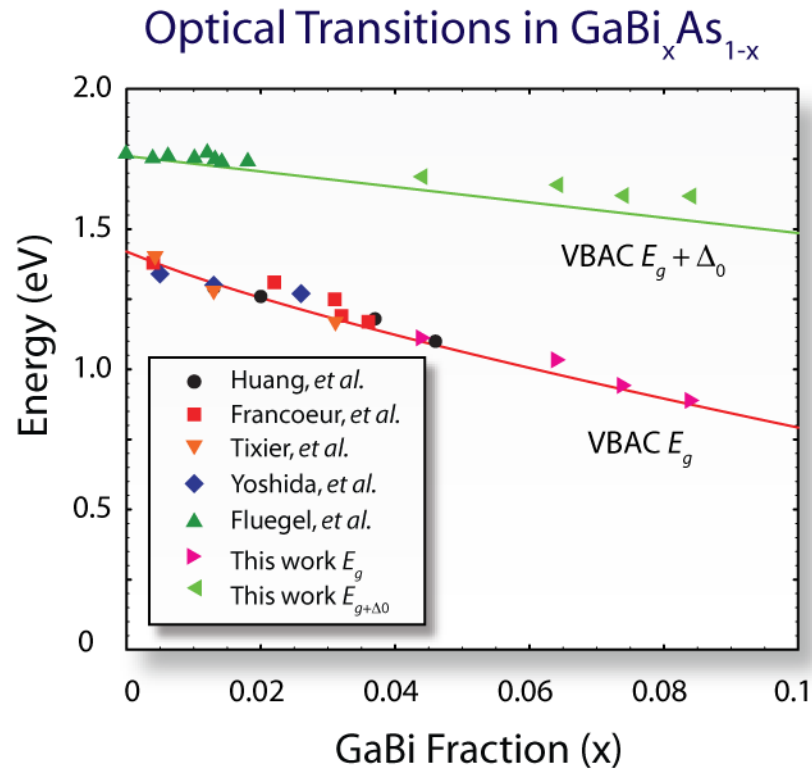
Optical Transitions



PR Spectra of $\text{GaBi}_x\text{As}_{1-x}$

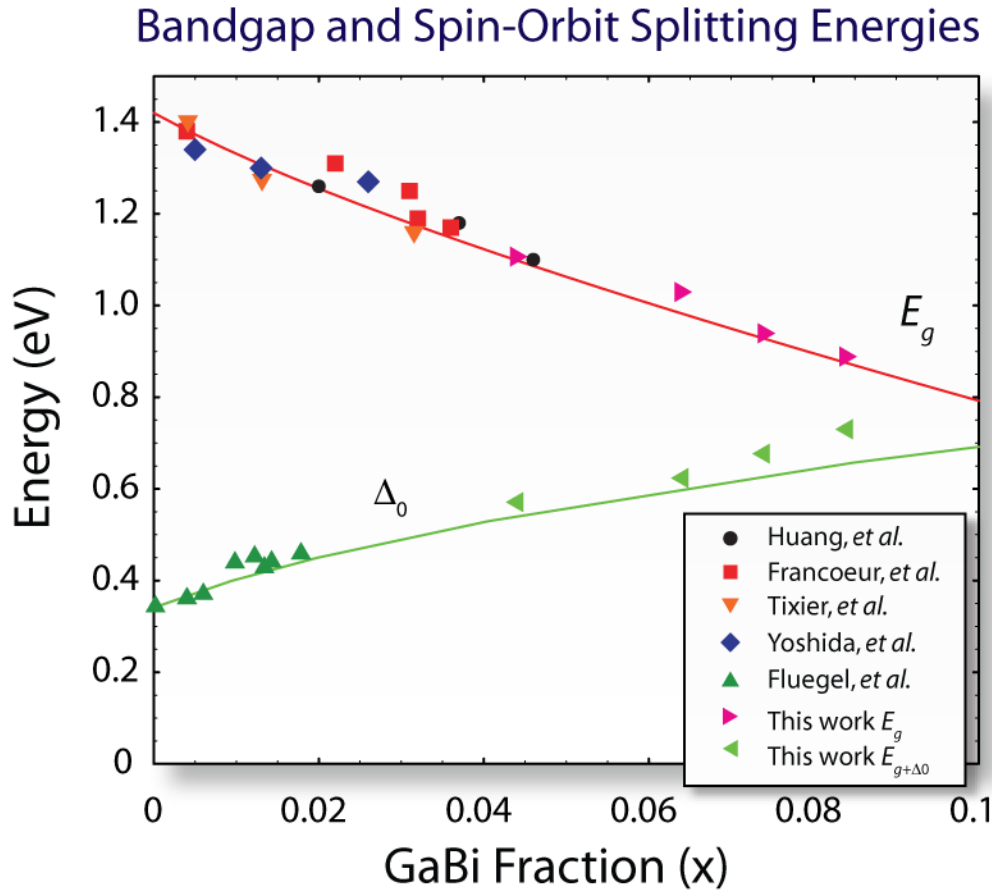


Restructuring of the Valence Band in $\text{GaBi}_x\text{As}_{1-x}$



Bandgap bowing in $\text{GaBi}_x\text{As}_{1-x}$ is due to the upward movement of the valence band edge

Bandgap and Spin Orbit Splitting Energies



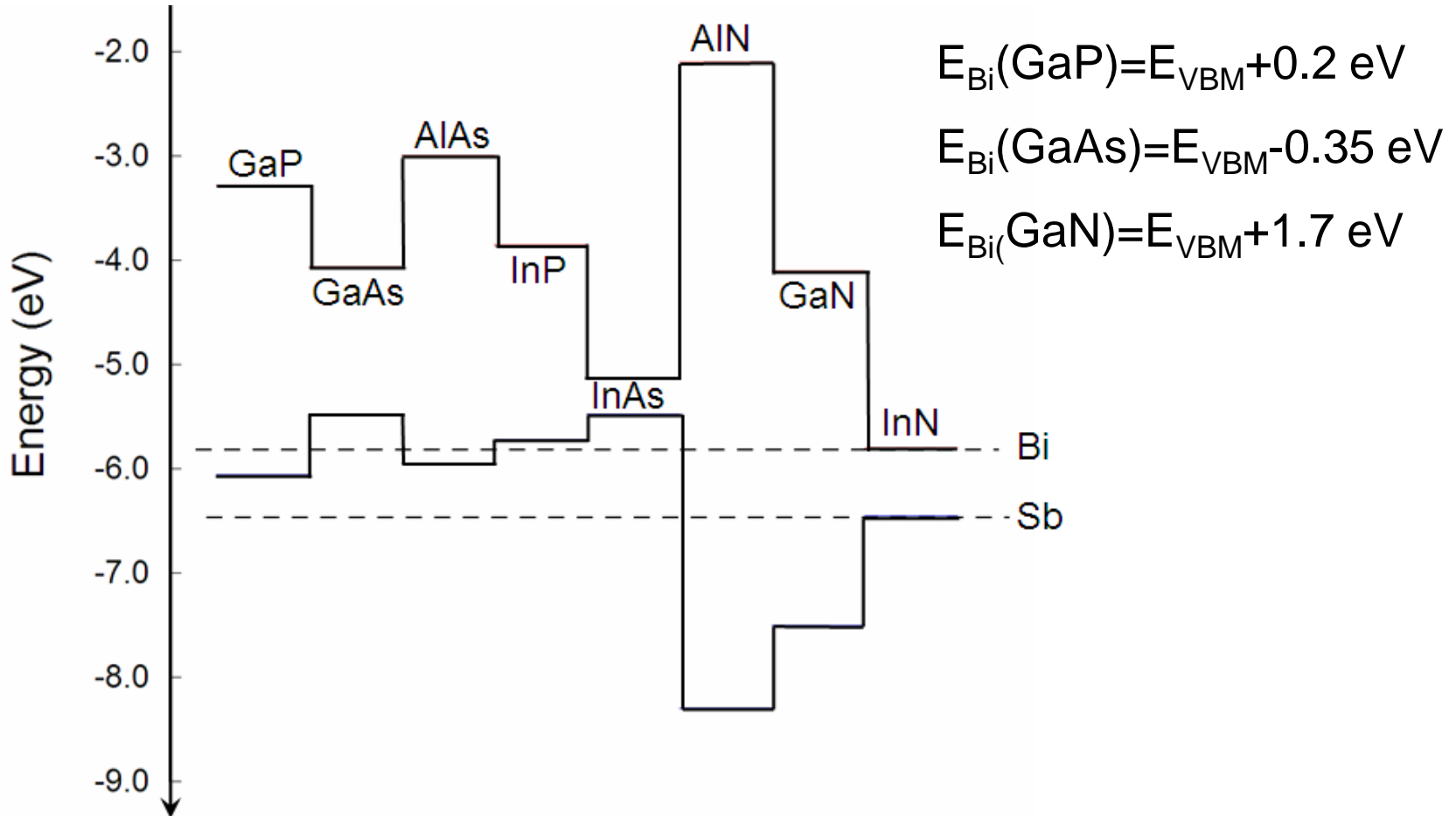
Bandgap Energy

Decreases by ~ 90 meV per $x = 0.01$

Spin-Orbit Splitting Energy

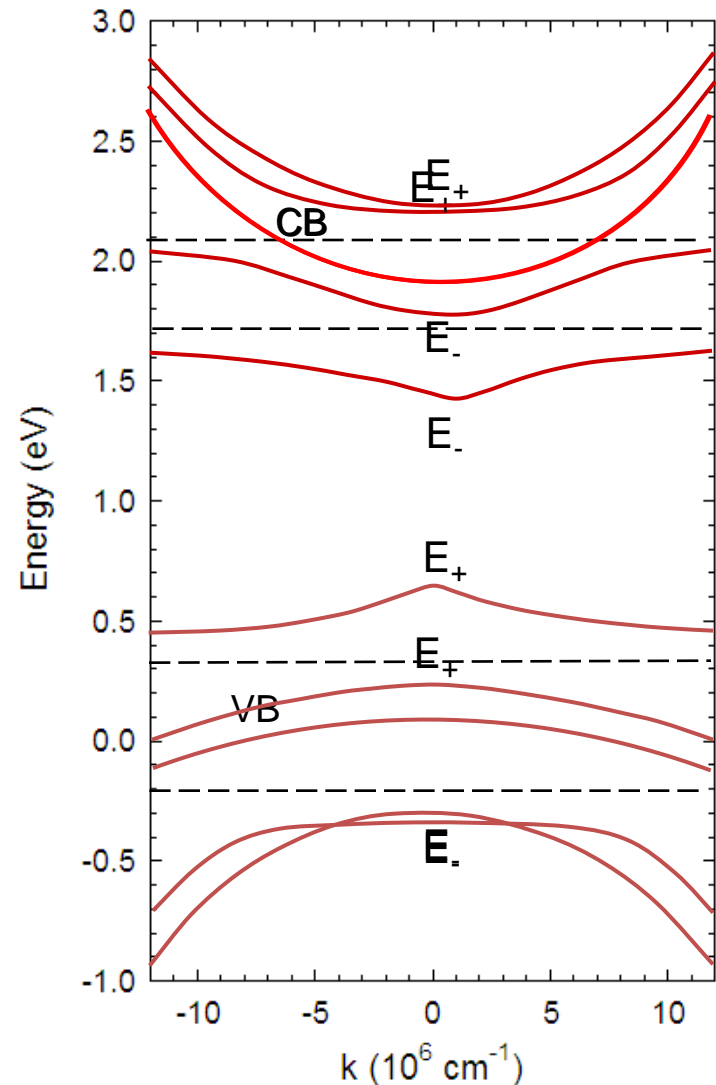
Increases by ~ 50 meV per $x = 0.01$

Bismuth in III-Nitrides: $\text{GaN}_{1-x}\text{Bi}_x$

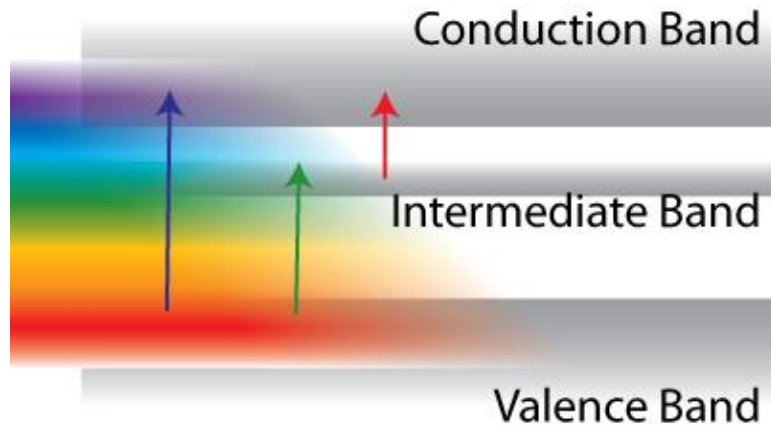


Band Structure Engineering of HMAs

- • Localized level above CBE and interaction with CB
 - GaAs(N), ZnSe(O), CdTe(O)
- • Localized level below CBE and interaction with CB
 - GaAsP(N), ZnTe(O)
- • Localized level above VBE and interaction with VB
 - GaN(As), GaN(Bi), ZnO(Se), ZnSe(Te), ZnS(Te), GaAs(Mn)
- • Localized level below VBE and interaction with VB
 - GaAs(Bi), GaAs(Sb), Ge(Sn)

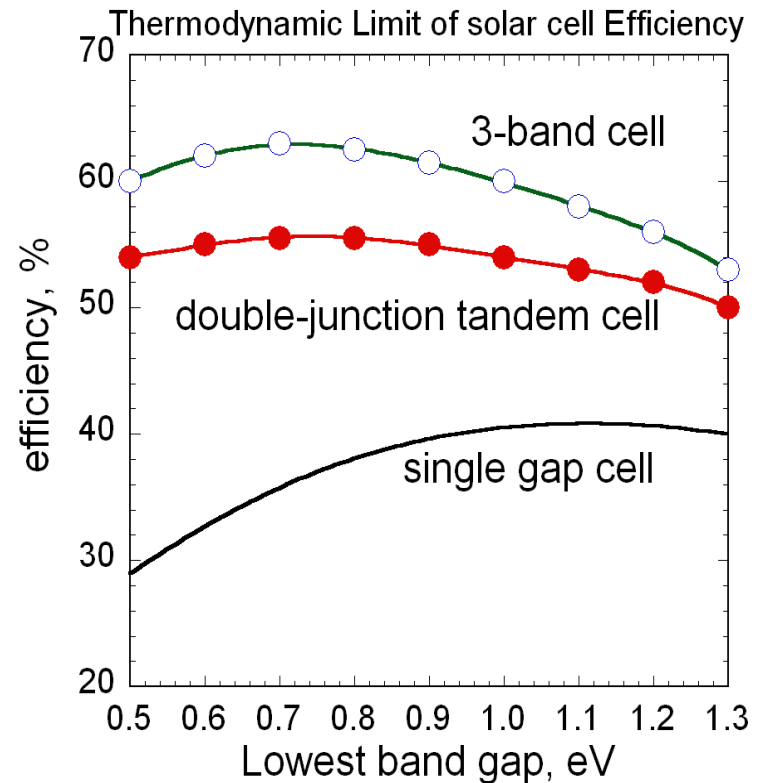


Highly Mismatched Alloys for Intermediate Band Cells



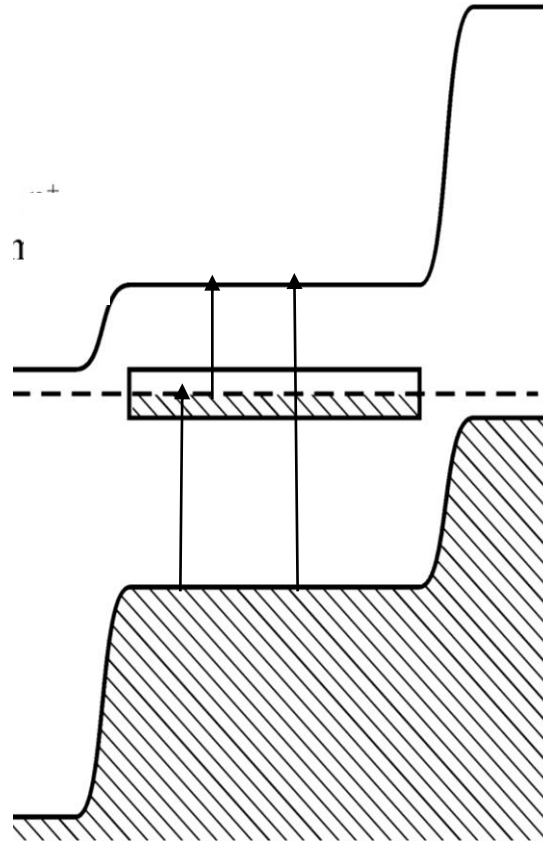
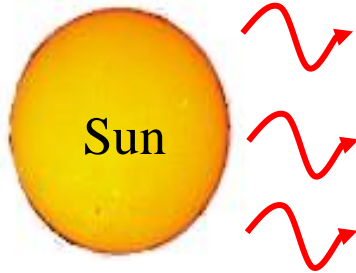
The intermediate band serves as a “stepping stone” to transfer electrons from the valence to conduction band.

Photons from broad energy range are absorbed and participate in generation of current.

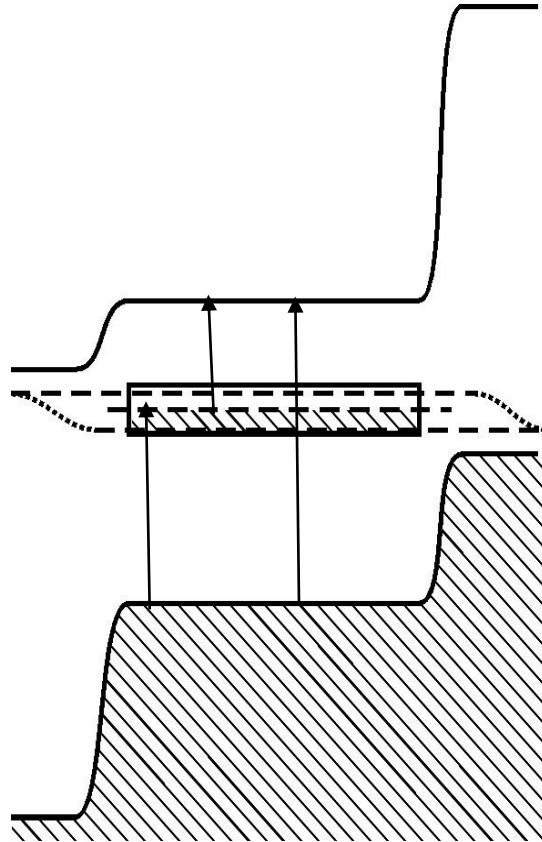
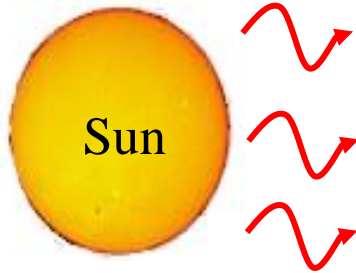


**Major technological advantage:
requires single p/n junction only**

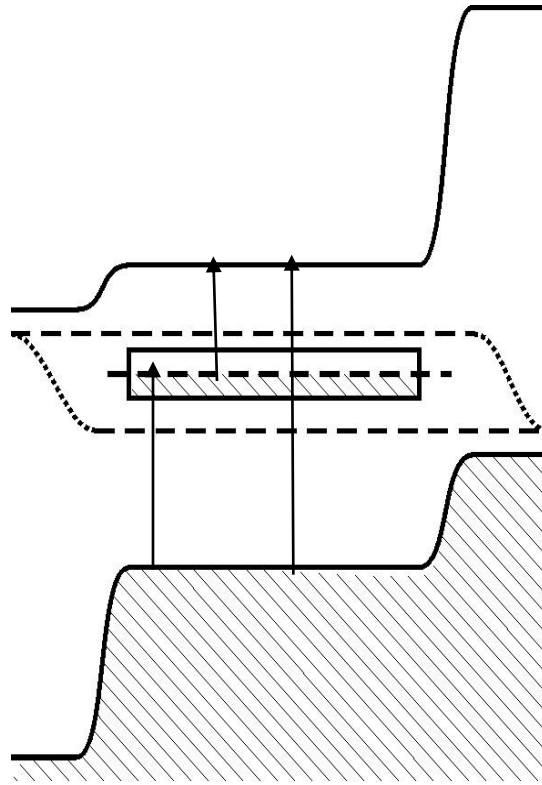
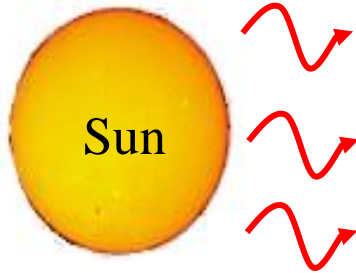
Intermediate band cell



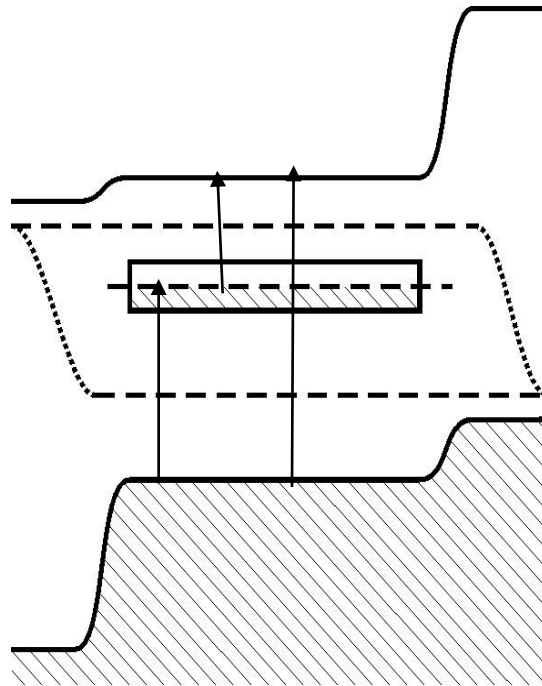
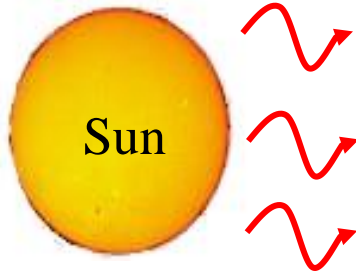
Intermediate band cell



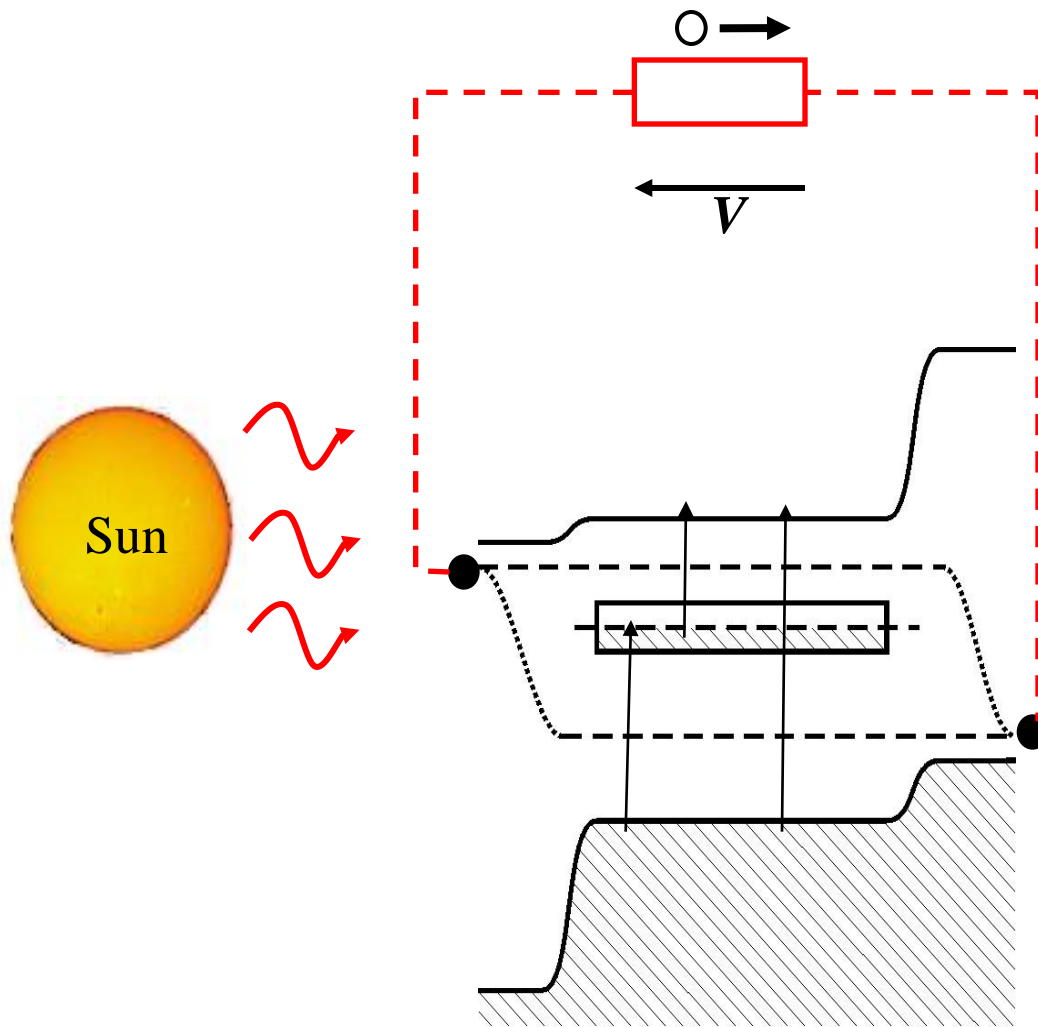
Intermediate band cell



Intermediate band cell

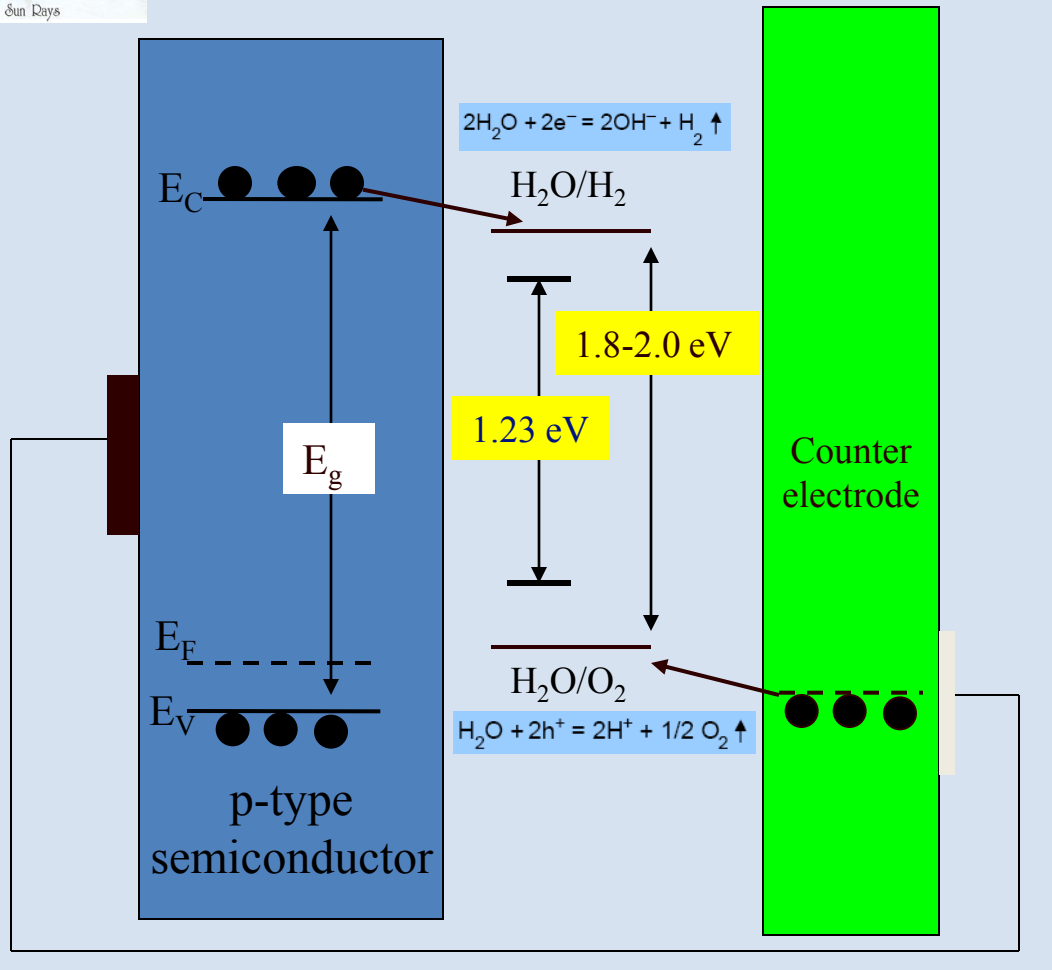


Intermediate band cell



Two small energy photons produce single electron-hole pair contributing to large V_{oc}

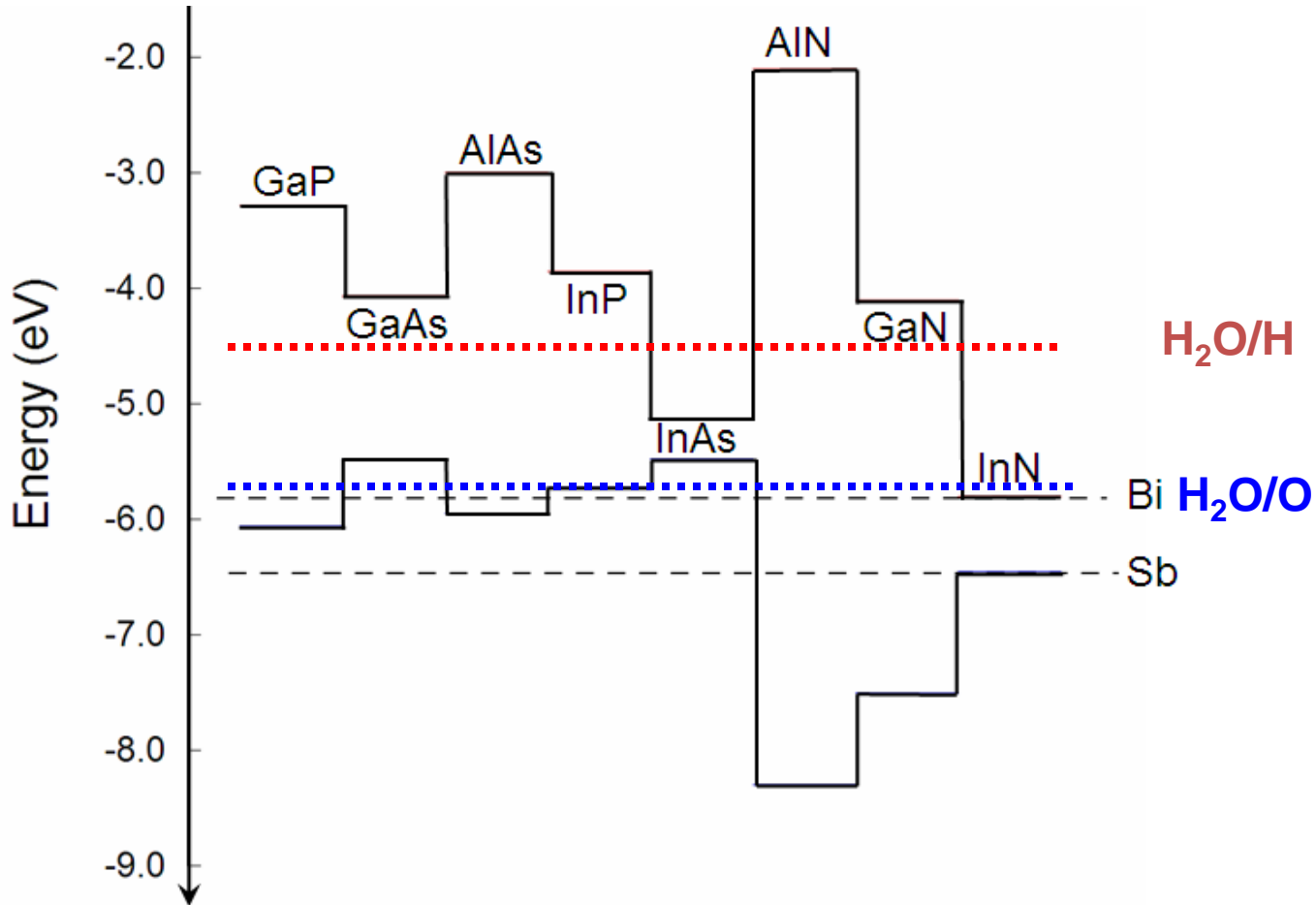
Photoelectrochemical Cells (PECs)



Material requirements

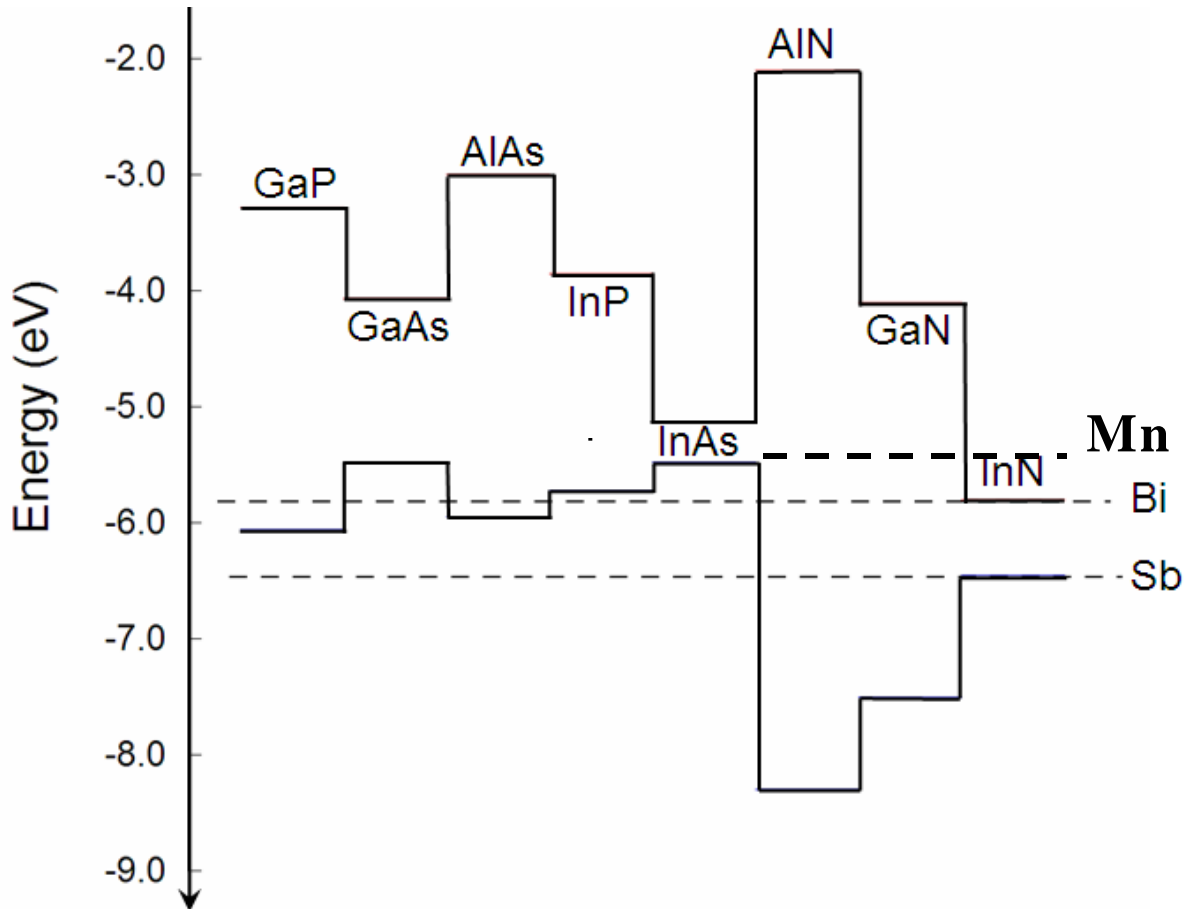
- Band gap must be at least 1.8-2.0 eV but small enough to absorb most sunlight
- Band edges must straddle Redox potentials
- Fast charge transfer
- Stable in aqueous solution

Group III-Nitride PECs ($\text{GaN}_{1-x}\text{Sb}_x$)



Bi level too high but Sb level lies low enough below oxygen redox potential $\text{H}_2\text{O}/\text{O}$

Ferromagnetic coupling in $\text{Ga}_{1-y}\text{Mn}_y\text{N}_{1-x}\text{Bi}_x$?



Energy level of the Mn impurity is expected to lie close to the Bi level.

Strong coupling between Mn holes and the Bi derived valence band

Conclusions and Outlook

Conclusions

- A large number of HMAs synthesized and studied.
- Electronic band structure described by the band anticrossing model.
- HMAs allow for an independent control of the location of CBE and VBE.
- Band anticrossing for electrically active impurities (III-Mn-Vs).

Outlook

- Potential applications for solar power conversion devices.
- HMAs for controlled ferromagnetic coupling.
- GaInNAs based photoelectrochemical cells.
- Energy selective contacts for hot electron solar cells.

Key role of highly mismatched III-Bi-V alloys